MICROCOPY   CHART

REPORT DOCUMENTATION PAGE

1. REPORT NUMBER	2. GOVT ACCESSION NO.	3. RECIPIENT'S CATALOG NUMBER
Technical Report #13		

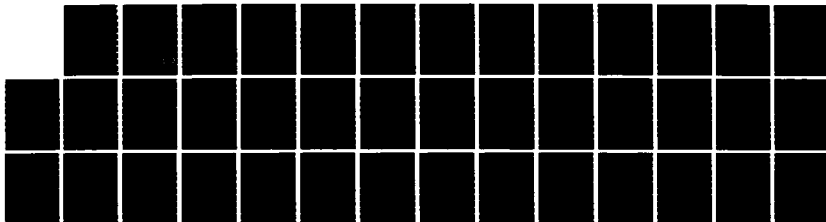| 4. TITLE *(and Subtitle)*	5. TYPE OF REPORT & PERIOD COVERED
CONTINUOUS PHASE TRANSITIONS IN TWO DIMENSIONAL SYSTEMS	Technical Report
	6. PERFORMING ORG. REPORT NUMBER

7. AUTHOR(s)	8. CONTRACT OR GRANT NUMBER(s)
W. N. Unertl	Contract #N00014-79-C-0441

9. PERFORMING ORGANIZATION NAME AND ADDRESS	10. PROGRAM ELEMENT, PROJECT, TASK AREA & WORK UNIT NUMBERS
Department of Physics and Astronomy University of Maine, Orono, ME 04469	Project #NR392-032

11. CONTROLLING OFFICE NAME AND ADDRESS	12. REPORT DATE
Office of Naval Research Physics Program Office Arlington, Va 22217	May 1986
	13. NUMBER OF PAGES
	39

14. MONITORING AGENCY NAME & ADDRESS *(if different from Controlling Office)*	15. SECURITY CLASS. *(of this report)*
	unclassified
	15a. DECLASSIFICATION/DOWNGRADING SCHEDULE

16. DISTRIBUTION STATEMENT *(of this Report)*

Approved for public release; distribution unlimited

17. DISTRIBUTION STATEMENT *(of the abstract entered in Block 20, if different from Report)*

18. SUPPLEMENTARY NOTES

A review article under contract with Comments on Solid State Physics

19. KEY WORDS *(Continue on reverse side if necessary and identify by block number)*

Surface phase transitions, chemisorption, reconstruction, statistical mechanics

20. ABSTRACT *(Continue on reverse side if necessary and identify by block number)*

See first paragraph

DD FORM 1473 EDITION OF 1 NOV 65 IS OBSOLETE
S/N 0102-014-6601|

CRITICAL PHENOMENA ON SURFACES:
RECONSTRUCTIONS AND CHEMISORBED LAYERS

W.N. Unertl

ABSTRACT

This article reviews recent experimental studies of the phase transitions which occur on reconstructed surfaces and in layers of chemisorbed atoms. Emphasis is given to systems which exhibit continuous transitions. The experimental results are presented in the context of current theories which emphasize the roles of symmetry, dimensionality and universality. The limitations currently imposed by sample quality and experimental techniques are also discussed. Results from individual systems are surveyed and promising future directions including studies of finite size effects are discussed.

1. INTRODUCTION

The concepts of symmetry, dimensionality and universality are central to contemporary theories of critical behavior. Indeed, some classes of transitions are predicted to occur only in two dimensional systems. This fact has led to an outburst of experimental activity to study critical phenomena on real surfaces. Second-order phase transitions have special importance in this context and the purpose of this review is to provide a survey of the extent to which recent experiments support current theoretical descriptions of second-order phase transitions.

Surface phase transitions are also of interest because they can effect such diverse phenomena as heterogeneous catalysis and thin film growth. Surface diffusion [1], adsorption and desorption rates [2], chemical reactions on surfaces [3], and the degree and type of order in thin films [4] are other examples of processes which can be influenced by phase transitions.

The equilibrium properties of a surface system are conveniently summarized on a phase diagram. This article is concerned only with closed systems; i. e. those for which the number of particles in the surface layer remains constant. The phases for closed systems are usually represented on a Temperature vs. Coverage (T vs θ) phase diagram. Figure 1 is a typical example, in this case for selenium adsorbed on the Ni(100) surface [5]. The ranges of T and θ over which the various phases exist are delineated by phase boundaries which can be either first- or second-order. The crystallographic structure of each phase and the precise location of its phase boundaries are determined by the interactions of adsorbate atoms with each other and with substrate atoms. Figures 2a and 2b show the atomic structure of the simple p(2 x 2) and c(2 x 2) phases of Figure 1. The sequence in which these phases are formed as θ increases provides direct information about the relative interaction strengths between Se atoms as shown in Figure 2c. For example, in the perfect p(2 x 2) phase, nearest-neighbor and next-nearest-neighbor adsorption sites are not occupied by Se atoms. Thus, the interaction E_3 must be more attractive than either E_1 or E_2. Since the c(2 x 2) phase forms next, E_2 must be more attractive than E_1. Therefore, we conclude that $E_3 < E_2 < E_1$. The numerical values of these energies can be estimated by fitting calculated phase boundaries to the experimental boundaries using various statistical mechanical techniques [5]. Such fits provide one of the few methods currently available for determining the interaction energies between adsorbed atoms. This is one of the major motivations for studying surface phase diagrams.

The variety of possible surface phase transitions is immense. This article is restricted to only a small subset of these: (1) phase transitions which occur on clean,

3

reconstructed surfaces (e.g. Au(110) (1x2) and W(100) c(2x2)), and (2) phase transitions in ordered layers of chemically adsorbed atoms. Other important systems include physisorbed layers [6], intercalation layers [7], liquid crystals [8] and lipid films [9]. Furthermore, we discuss only systems for which the phase diagram and its phase boundaries have been experimentally determined. Finally, only adsorption systems which can reasonably be described by lattice gas models are included; i. e. those for which adsorption is at specific sites on the surface. Thus, commensurate-incommensurate transitions and sequences of compressed phases are outside the scope of this article [10].

The experiments discussed here rely entirely on Low Energy Electron Diffraction (LEED) to characterize the degree of order. The reader is assumed to be familiar with the basic ideas of diffraction theory and the reciprocal lattice [11,12] and to have a working knowledge of the notation used to describe two dimensional, periodic structures [13].

2. THEORETICAL BACKGROUND

This section summarizes some of the basic theoretical background needed to place the experimental studies of continuous order-disorder phase transitions into the context of modern theories of critical behavior. Since this presentation must be brief, references are given throughout to more detailed treatments.

2.1 Order Parameter, Pair Correlations and Correlation Length

Three measurable quantities whose behaviors in the vicinity of a phase transition are predicted by theory are the order parameter, the pair correlation function and the correlation length. Consider, for example, the case of a lattice gas of particles adsorbed on a lattice with unit mesh vectors a_1 and a_2 and lattice sites at $r_i = m_{1i}a_1 + m_{2i}a_2$ where m_{1i} and m_{2i} are integers. At any instant the probability n_i that a particular site r_i is occupied is either one or zero; $n_i = 0,1$. The average occupation probability $\langle n_i \rangle$ is given by the average of all possible configurations of the particles each weighted by its statistical probability [14]. As the degree of order changes near a phase transition, $\langle n_i \rangle$ also changes.

The order parameter ϕ_j is a function (or set of functions) that describes the average degree of order at each site on the lattice as a function of temperature. In diffraction, the ϕ_j are most conveniently defined in terms of the Fourier coefficients of the average site occupation probability $\langle n_i \rangle$. The number of components j of the the

4

order parameter is equal to the number of terms in this expansion. Consider the example in Figure 3. Figure 3a shows a (2x1) structure on a square lattice which has a two component (vector) order parameter. In this case there are two symmetry equivalent orientations of the (2x1) structure. The order parameters associated with these possibilities are

$$\phi_1 = \frac{1}{N} \sum_j \langle n_j \rangle e^{i k_1 \cdot r_j} \qquad \text{(1a)}$$

and

$$\phi_2 = \frac{1}{N} \sum_j \langle n_j \rangle e^{i k_2 \cdot r_j} \qquad \text{(1b)}$$

where N is the number of lattice sites, $k_1 = a_1^*/2$ and $k_2 = a_2^*/2$ are reciprocal lattice vectors characteristic of each possible (2 x 1) lattice as shown in Figure 3b and a_1^* and a_2^* are the reciprocal lattice unit mesh vectors of the substrate. For a perfect (2x1) phase $\phi_1 = 1/2$. A c(2x2) phase, Figure 2b, on this same substrate lattice is described by the reciprocal vector q and has a single component (scalar) order parameter

$$\phi_3 = \frac{1}{N} \sum_j \langle n_j \rangle e^{i q \cdot r_j}. \qquad \text{(1c)}$$

The pair correlation function $\langle n_i n_j \rangle$ provides more detailed information about the ordering than does ϕ since $\langle n_i n_j \rangle$ gives the probability that the lattice sites at r_j and r_i are simultaneously occupied. Since n_i can be written as a sum of its average value $\langle n_i \rangle$ and its instantaneous fluctuation δn_i from that average, one obtains

$$\langle n_i n_j \rangle = \langle n_i \rangle^2 + \langle \delta n_i \delta n_j \rangle. \qquad \text{(2)}$$

The functional form of $\langle \delta n_i \delta n_j \rangle$ is such that it decreases as r_i and r_j become farther apart. The length which characterizes this fall-off is called the correlation length ξ and is a measure of the distance over which fluctuations from the average coverage are $\langle n_i \rangle$ correlated. Higher order correlation functions can also be defined but little is known about their properties for real systems.

2.2 Diffraction from a Disordered Lattice

If a perfect two-dimensional lattice is illuminated by radiation with wavevector k_0 ($|k_0| = 2\pi/\lambda$, where λ is the wavelength), diffracted beams are observed only at scattered wave vectors k which satisfy the Laue conditions [11,13]. If disorder is introduced onto the lattice, intensity is removed from the beams and redistributed throughout space. In this case, the averaged intensity scattered from the lattice is

$$I = |f(k,k_0)|^2 (I_{LRO} + \chi(S)) \qquad (3)$$

where $|f(k,k_0)|^2$ is the differential scattering cross section and $S \equiv k - k_0$ is the scattering vector [13]. Only $S_{||}$, $k_{0||}$ and $k_{||}$, the components of S, k_0 and k, which are parallel to the plane of the lattice are important. Equation (3) neglects any multiple scattering; these contributions can be included by adding terms which include higher-order correlation functions [15]. I_{LRO}, the first term in (3), is just the scattered intensity that would be obtained for a perfect lattice with a particle at every lattice site but reduced by the factor ϕ^2; i.e.

$$I_{LRO} \equiv \phi^2 \, \delta(S_{||} - G_{hk}) \qquad (4)$$

where G_{hk} are the reciprocal lattice vectors of the two dimensional lattice. $\chi(S)$, the second term in (3) is due to fluctuations:

$$\chi(S) = \sum_{ij} \langle \delta n_i \delta n_j \rangle e^{iS \cdot r_{ij}} \qquad (5)$$

In analogy with magnetic systems, $\chi(S)$ is called the susceptibility. $\chi(S)$ is a peaked function and its half-width $\Delta S_{||}(1/2)$ is inversely related to the correlation length ξ by

$$|\Delta S_{||}(1/2)| = 2\pi/\xi. \qquad (6)$$

For the case of continuous phase transitions, the susceptibility is often approximated as a Lorentzian function [16,17].

6

2.3 Critical Exponents and Universality

The modern theory of continuous phase transitions postulates that certain entities called critical exponents provide a meaningful description of a system near a critical point. For example, if $F(T)$ is some physical quantity of interest such as the order parameter, its variation near the critical temperature can be described by

$$F(t) \simeq F_0 |t|^{\omega} + \dots \qquad (7)$$

where ω is the critical exponent, $t \equiv (T - T_c)/T_c$ is the reduced temperature and F_0 is an amplitude. Higher-order terms in (7) are unimportant as long as t is near enough to zero. Originally it was hoped that the critical exponents would have a single set of values [17]. However, in reality there seem to be several distinct sets which apparently depend upon the dimensionality of the system and the symmetry of the order parameter [17]. Each set is called a Universality Class. The important universality classes for two-dimensional systems are listed in Table 1. The critical exponents which can be determined by a diffraction experiment are also listed. Table 2 contains a compilation of critical exponents which have been extracted from experimental data from reconstructed clean surfaces and chemisorbed layers.

The temperature dependence of the order parameter is described by the critical exponent β;

$$\phi(t) \simeq \phi_0 |t|^{\beta} + \dots \quad T < T_c$$
$$\qquad\qquad (8)$$
$$= 0 \qquad T > T_c .$$

The exponents γ and υ describe the behavior of $\chi(\Delta S_{||}, t)$, equation (5). The amplitude $\chi(0,t)$ obeys

$$\chi(0,t) \simeq \chi_0 |t|^{-\gamma} + \dots \qquad (9)$$

and the correlation length is given by

$$\xi(t) \simeq \xi_0 |t|^{-\upsilon} + \dots \qquad (10)$$

where ξ_0 is of the order of a lattice spacing.

7

Figure 4 is a schematic illustration of the variation of I_{LRO} and $\chi(S_{\parallel},t)$ near T_c predicted by equations (8) to (10). I_{LRO} falls continuously to zero at T_c while $\chi(0,t)$ has a singularity at T_c and decreases smoothly on both sides. Far below T_c only the δ-function I_{LRO} contributes to the line profile. As T increases toward T_c, I_{LRO} decreases and $\chi(S_{\parallel},t)$ becomes significant. At $T \ll T_c$, $\chi(S_{\parallel},t)$ is low and broad but it increases in magnitude and sharpens until at T_c it is the only contribution to the line profile. As T increases above T_c, $\chi(S_{\parallel},t)$ again decreases and broadens. Thus, an accurate measurement of the diffraction line profile as a function of temperature near T_c can be analyzed to obtain β, γ and υ. This is the theoretical basis of most studies of second-order phase transitions.

The critical exponent α is traditionally associated with the specific heat anomaly

$$C \cong C_0|t|^{-\alpha} + \dots . \qquad (11)$$

As recently pointed out by Roelofs, Einstein and Bartelt [15], α also describes the behavior of the "integrated" diffraction intensity according to the relation

$$I_{int}(t) = A_0 + A_1 t \pm B_{\pm}|t|^{1-\alpha} + \dots \qquad (12)$$

where $I_{int}(t)$ is the integral of the intensity profile over a small range of $\Delta S_{\parallel}$ values near the center of the Brillouin zone; i.e. at $S_{\parallel} = G_{hk}$. This result is valid as long as t is close enough to zero so that $\Delta S_{\parallel}$ is larger than the width of the susceptibility $\Delta S_{\parallel}(1/2)$. Equation (12) relies on the fact that a poor LEED instrument is sensitive predominantly to short-range order. This observation is extremely important because it opens the quantitative study of critical behavior to researchers with standard commercial instruments. Furthermore, equation (12) is valid even when multiple scattering, which is neglected in equation (3), is important.

2.4. Critieria for a Continuous Order-Disorder Phase Transition: Landau Theory

By 1937, Landau had recognized the role of symmetry in continuous order-disorder phase transitions [18]. In Landau's theory, the thermodynamic potentials $\Phi(\theta,T;\phi)$ are expanded in powers of the order parameter $\phi(\theta,T)$ in the vicinity of the critical point:

$$\Phi(\theta,T;\phi) = \Phi_0(\theta,T) + a(\theta,T)\phi + A(\theta,T)\phi^2 + B(\theta,T)\phi^3 + D(\theta,T)\phi^4 + \dots \qquad (13)$$

8

where a(θ,T), A(θ,T), B(θ,T) and D(θ,T) are temperature and coverage dependent coefficients which can themselves be expanded in powers of t near the critical point. The order parameter ϕ is also a function of θ and T and is determined by minimizing $\Phi(\theta,T)$ at particular θ and T. Landau and Lifshitz [19] determined the properties of the coefficients of equation (13) by applying a set of four symmetry rules which are now known as the Landau-Lifshitz Rules [20] and are discussed in detail in References 19 - 22.

The Landau-Lifshitz rules make it possible to find all possible second-order phase transitions (except commensurate-incommensurate transitions) without knowledge of the detailed mechanism of the ordering process. The rules however do not prove that a given system will actually have a second-order transition, only that such a transition is possible.

Landau theory has been applied to two dimensional systems and a complete classification of all possible order-disorder phase transitions has been made [21,22]. These are summarized in Table 1.

The procedure for predicting the universality class for a particular system is straightforward. First, the components of the order parameter must be identified. The Hamiltonian of the system is then expanded in terms of these components and the Landau-Lifshitz rules applied. The resulting, symmetrized Hamiltonian is called the Landau-Ginzburg-Wilson (LGW) Hamiltonian. This LGW Hamiltonian is then compared with the LGW Hamiltonians of the known universality classes [20-22] in order to identify the correct universality class. Examples are given in references 20-23.

Landau theory cannot be applied too near the critical line (θ_c,T_c) since the expansion of $\Phi(\theta,T;\phi)$ in equation (13) diverges there. However, as long as the root-mean-square fluctuations of ϕ averaged over the area ξ^2 are small compared to its average value, the arguments given above are expected to hold. Ipatova and Kitaev [20] have pointed out that this condition is more easily met in diperiodic three dimensional systems than in two dimensional systems. They suggest that diperiodic systems may provide an alternative approach for real surfaces.

2.5. Finite Size Effects.

The characterization of continuous phase transitions outlined above is only precise when the substrate lattice is perfect; e.g. semi-infinite in extent and free of imperfections. At best, this requirement can only be approximately satisfied by real surfaces since imperfections due to substrate mosaic structure, steps, dislocations

and impurities are always present. The influence of imperfections on the critical properties are called *finite size effects*.

Usually, finite size effects become important whenever the temperature is close enough to T_C that the correlation length ξ becomes comparable to the spacing between imperfections. At this point the imperfections begin to influence the fluctuations and alter the critical exponents in equations (8)-(12). The effective critical temperature is also altered [24,25]. The surfaces of real single crystals are usually only free of imperfections on the scale of several tens of nanometers and finite size effects are important. Quantitative descriptions of the way in which finite size effects influence critical behavior have only been developed for a few special geometries and considerable theoretical work is still needed. Kleban [23] has recently reviewed the status of this area.

3. EXPERIMENTAL METHODS

Experimental characterization of an order-disorder phase transition in a real surface system is not simple for several reasons. Sample preparation is difficult and not well-developed. Accurate <u>absolute</u> measurement and control of substrate temperature and adsorbate coverages is very difficult. The time available for measurements is often severely limited by the need to avoid surface contamination due to adsorption of residual gases. The response of the instrument distorts the measured line profiles and limits the sensitivity to long-range-order. Other processes also contribute to changes in the line profile and are not easily accounted for in the analysis. These include scattering from impurities, extended surface defects, the bulk mosaic structure and thermal vibrations. Furthermore, in the case of LEED, multiple scattering is a major contributor to the total intensity.

Despite this long list of experimental concerns, numerous successful measurements have been completed and substantial progress is being made to overcome most of these outstanding problems.

3.1 Sample Preparation and Surface Imperfections.

The methods currently used to prepare oriented, single crystal surfaces are not highly developed. They are based on standard metallographic practices [26] and typically include mechanical, chemical and/or electrochemical polishing sequences. Crystallographic orientation is usually determined with the aid of X-ray Laue back reflection photographs. Since this method is only accurate to about $\pm 0.2°$, a typical

10

surface has atomic height steps separated on average by not more than a few tens of nanometers. Surfaces of this quality are only marginally suited for studies of long-range-order. More accurate X-ray orientation procedures requiring measurement of line profiles and relative intensities can significantly reduce the degree of misorientation to less than 0.05° [27] and need to be more widely employed. Surface polishing procedures also need to be more carefully developed to minimize degree of surface disorder.

The surface cleaning procedures employed inside the ultra-high vacuum analysis chamber also have considerable potential for introducing surface imperfections. The "standard" method is sputter cleaning by bombardment with energetic inert gas ions. Sputtering is a violent process and creates extensive damage usually in the form of randomly distributed step arrays but sometimes also creates irreversible macroscopic changes including formation of cones [28]. The degree to which vacuum annealing restores a defect free surface is not well understood. Chemical cleaning processes [29] involving reaction with gases are intuitively appealing but no studies of their effects on the surface long-range- order have been made. Unfortunately, chemical reactions may not be able to remove all impurities.

Surface spectroscopy techniques such as Auger electron spectroscopy [13,30] seldom have practical sensitivities better than about 0.1% of a monolayer. Thus, the mean separation of surface impurities can easily be smaller than 10 nanometers. Adsorption of impurities from the residual gas is also an important source of contamination for many materials. For example, for a pressure of 10^{-12} Torr and unity sticking probability, less than one-half hour is required to accumulate about 0.1% of a monolayer of impurity. This corresponds to an impurity atom separation of about 7-8 nm.

The extent to which uncontrolled defects and impurities influence studies of critical phenomena by introducing finite size effects is not known at present. The improved diffraction equipment needed to better characterize the starting surface is only just becoming available [31].

Studies of critical behavior of chemisorbed layers on surfaces have relied on Auger electron spectroscopy (AES) to determine the relative surface coverage of the adsorbate. For submonolayer coverages, the AES signal is directly proportional to the coverage as long as the electronic structure of the adsorbate does not change drastically with coverage. Thus, the relative coverage can be determined with high accuracy. However, AES cannot measure the absolute coverage to better than twenty or thirty percent so that another method is always needed to calibrate the coverage scale. This method has been LEED in all of the experimental studies of overlayer

critical phenomena discussed in the next section. For example, the coverage scale in Figure 1 was set by assuming that the half-order diffraction beams of the p(2 x 2) phase reach maximum intensity at precisely one-quarter monolayer [5]. This method can easily be in error by five to ten percent. Kinetic effects may limit the removal of domain boundaries. Adsorption near impurities and defects may have different properties than on the perfect surface [23,32]. Even absolute methods such as nuclear reaction analysis [33] and x-ray fluoresence [34] are not more accurate than a few percent. Fortunately, for many properties of interest, it is sufficient to know only relative coverages.

Imperfections give rise to finite size effects which limit the smallest value of t for which the power law behavior given in equations (8) - (12) will be valid. The smallest value of t attained so far is about 0.005 [35]. This has the consequence that only very small ranges of t have been used to test equations (8) - (12), typically about one order of magnitude. Thus, at present, surface imperfections provide one of the most significant limitations to our ability to test universality in model two-dimensional systems.

3.2 Diffraction Instrumentation

Low-Energy Electron Diffraction (LEED) is the only technique that has been used to study critical phenomena at continuous order-disorder transitions for systems of interest in this review. Atom diffraction [36] and X-ray Diffraction [37] would also be suitable but have not yet been employed. In LEED, not only do sub-surface atomic layers contribute to the signal but multiple scattering effects may be too large to be ignored [38,39]. This makes complete analysis of LEED intensities complex.

An ideal instrument would illuminate the sample with a plane wave of monochromatic radiation and the detector would accept only elastically scattered radiation with a specific wavevector $\mathbf{k}$. Real instruments do not meet these requirements [40]. Deviations from ideal behavior can be described by the instrument response function T(S) [41]. If I(S) represents the diffracted intensity in the absence of instrumental effects, then the measured intensity J(S), is given by

$$J(S) = T(S) * I(S) \qquad (14)$$

where * represents a convolution product. In principle, most features of T(S) can be determined experimentally if a sufficiently perfect crystal is available and the

determination is carried out at a temperature which is low enough that thermal diffuse scattering due to phonons is negligible.

$T(S)$ is often characterized by its Fourier transform $t(R)$; $t(R)$ is peaked at $R = 0$ and falls off to zero at large R. The transfer width $R_{1/2}$ is the full-width at half-maximum of $t(R)$ and is used as a measure of the degree to which a particular diffractometer is sensitive to long-range-order. For an ideal instrument, $R_{1/2}$ would be infinite but for most LEED instruments currently in use, $R_{1/2}$ is small, typically in the range 5-20 nm. Since, correlation lengths can be several hundred Angstroms in two-dimensional systems [6], a small value of $R_{1/2}$ can make it difficult to distinguish certain types of fluid from solids. Recently, several new LEED diffractometer designs have been realized and provide substantially improved instrumental resolution [31,40].

Whenever the correlation length ξ is comparable to $R_{1/2}$, it is essential that the effect of $T(S)$ on the measured line profile be included in the analysis. Ideally, this would be done by direct deconvolution of equation (14) to extract $I(S)$, however this is difficult in practice both because of uncertainties in the measured $T(S)$ and because of the finite range of S over which it can be determined. Instead, the normal procedure is to assume that the width of a profile measured far below T_C is entirely due to the instrument response. In the vicinity of T_C, the measured profile may then be fit by assuming a particular form for the fluctuation contribution $\chi(S_{\parallel},t)$, equation (5); usually $\chi(S_{\parallel},t)$ is taken to be Lorentzian [16]. The amplitude χ_0 and width $\Delta S_{\parallel}(1/2)$ of the Lorenztian plus the intensity of the low-temperature line profile are used as adjustable fitting parameters. The temperature dependence of each of these parameters is then fit to equations (8)-(12), to determine the critical exponents. A constant term is usually included in the analysis to approximately account for a "background".

3.3. Additional Considerations.

There are several additional factors which can change the shape or temperature dependence of a line profile. For example, the experimental configurations normally employed do not measure the diffraction line profile along $S_{\parallel}$, but along some curved trajectory in reciprocal space [42]. This can result in an underestimate of $\Delta S_{\parallel}(1/2)$ by as much as fifty percent and thus in an overestimate of the correlation length ξ.

In addition, the equations presented in Section 2 do not incorporate the effects of all physical processes which contribute to the diffracted intensity and its line profile.

13

One of these is the temperature dependence due to the Debye-Waller factor e^{-2M} which is a function of both S and T;

$$2M = \langle(S \cdot u)^2\rangle$$

where **u** is the root-mean-square vibrational amplitude of the surface atoms and is proportional to T in the high temperature limit. 2M can be determined experimentally from the slope of ln I vs. T measured for T far away from T_c. It is typically in the range 0.5-3.0 for most materials and is a substantially larger correction for surfaces than for the bulk not only because of the larger vibrational amplitudes of surface atoms but also because of the absense of translational symmetry normal to the surface [43,44].

The intensity removed from a diffraction beam by the Debye-Waller factor is redistributed throughout the Brillouin zone as one- and multi-phonon thermal diffuse scattering (TDS) [43,44]. The intensity of the one-phonon scattering has its maximum near the Bragg peak. This additional peaked intensity can cause the measured line width to be increased by twenty to thirty percent [42]! The effects of TDS increase at higher T and for large values of S. No experimental analysis of critical behavior has yet attempted to include the effects of TDS.

Multiple scattering is very strong for low energy electrons and diffracted intensities cannot be calculated using the single scattering theory as assumed in the derivation leading to equation (3). Consequently, one must ask whether multiple scattering can alter the line profiles sufficiently to invalidate the use of equation (3) for the analysis of real LEED data. Unfortunately, we do not have clear answer to this question at the present time. At least some experiments have attempted to use diffraction conditions which might minimize the contributions of multiple scattering. However, the fact that critical phenomena are studied using non-specular beams means that at least two Bloch waves can be excited and must be treated self-consistently in any analysis [45]. Recent results of conformal mapping analysis indicate that multiple scattering might even dominate the line profiles at T_c [46]. A recent theoretical analysis by Moritz and Lagally [39] suggests that multiple scattering cannot be ignored. However, Bennett and Webb [47] have made line profile measurements on several beams and they found consistent results. Since the relative contributions from multiple and single scattering will vary strongly from diffraction beam to diffraction beam, this result gives some support for neglect of multiple scattering in line profile analysis. Comparison of profiles measured for the same system with both LEED and with X-ray diffraction could directly test for the

14

importance of multiple scattering because X-ray intensities are described by the single scattering theory. Such measurements are planned [48].

Finally, it should also be pointed out that the method of Bartelt, Roelofs and Einstein [15] for determination of the specific heat critical exponent α does not seem to be sensitive to multiple scattering effects. This fact makes this method additionally attractive to the experimentalist.

4. EXPERIMENTAL STUDIES OF CRITICAL BEHAVIOR.

Davisson and Germer probably made the first observation of a surface order-disorder transition in their classic paper on electron diffraction [49]. The first modern observation was by McRae for O on Ni(100) [50]; this system was later shown to be complicated by the onset of O dissolution into the bulk for $T \sim T_c$ [51]. Perhaps the first experiment designed specifically to study a surface order- disorder transition was a LEED study made on $Cu_3Au(100)$ by Sundaram et al. [52].

Only a few careful studies of critical behavior on clean and chemisorbate covered surfaces have now been carried out. These are reviewed in this section.

4.1. Reconstructions on Clean Surfaces.

4.1.1. Au(110)(1x2): Realization of the Ising Universality Class.

The first attempt to extract a critical exponent for a surface system was made by Wolf et al. [53] for the Au(110)(1x2) order-disorder transition. Although they corrected the data for the instrument response function, they did not include critical fluctuations in the analysis. This resulted in a larger value for β than currently accepted for this system.

A complete analysis of this transition was made by Campuzano et al. [16] and confirmed the earlier prediction by Bak [54] that the transition should be in the simple Ising universality class. The line profiles of the (10), (1,-1/2) and (1,$\bar{1}$) beams were measured along the <01> direction as a function of temperature for normally incident, 20 eV electrons. The line profile measured in the fully ordered (1x2) phase for $T \ll T_c$ is a measure of I_{LRO}, equation (4), and could be fit by a Gaussian plus a uniform background term. The width of this Gaussian was substantially larger than that of the instrument response function and indicated that finite size effects limited the extent of the (1x2) surface long-range order to less than 15 nm. After correction for the measured Debye-Waller factor, the experimental line profiles were fit at each

15

temperature by assuming them to be a linear combination of I_{LRO} and the susceptibility $\chi(S_{||},t)$, equation (5), plus a uniform background. The critical exponents β, γ and ν were extracted from the temperature dependence of I_{LRO}, χ_0 and $\Delta S_{||}$ respectively assuming the forms in equations (8)-(12). The resulting fits are shown in Figure (5a) and the exponents are tabulated in Table 2. T_c was found to be 650 ± 7 K.

The consequences of finite size effects due to the limited perfection of the (1x2) phase are reflected in both $I_{LRO}(T)$ and $\chi_0(T)$ as shown in Figure 5b. I_{LRO} decreases slightly less steeply than predicted by the classical Onsager model [55]. This causes the exponent β to be slightly larger than the predicted value. $\chi_0(T)$ is clearly peaked above T_c in a way similar to that predicted by Fisher and Burford [56]. As shown in Table 2, the measured exponents are in good agreement with the predicted values except for β which is slightly too large.

Clark et al. [35] have measured the exponent of the specific heat anomaly to be α = 0 ± 0.05. They used the method proposed by Bartelt, Einstein and Roelofs [15] which exploits the fact that the integrated intensity measured by a poor LEED instrument has lost its sensitivity to long-range order and is described by equation (12). They found the critical temperature to be 690 ± 7 K, a value that is higher than that reported Campuzano et al. [16]. This difference is due to the substantially better surface order of the crystal used by Clark et al. and is in good agreement with theoretical predictions for the Ising model [24,25].

Because Au(110) is inert to the background gases normally found in ultra-high vacuum systems, very long times are available for measurements. Thus, Au is expected to be a good model system for more extensive studies of continuous order-disorder transitions in two dimensions. Finite size effects can be introduced by using stepped surfaces or intentionally adding impurities. The role of multiple scattering and other corrections to the data such as TDS can be explored in detail. Studies of the kinetics of ordering will also be possible since the time scale over which the ordering takes place is reasonably slow.

The clean Ir(110) and Pt(110) surfaces also have a (1x2) reconstruction [57] and are thus expected to have order-disorder transitions which belong to the Ising universality class. Experiments to confirm this prediction remain to be carried out.

4.1.2. W(001)c(2x2): The XY Model with Cubic Anisotropy.

The clean W(001) surface reconstructs to a c(2x2) phase with a critical temperature of 211 K [57-59]. The diffraction pattern of the c(2x2) phase has p2mg symmetry due to small displacive translations of W surface atoms along <11> and <1 1̄>

16

directions. Since the unreconstructed (1x1) surface has p4mm symmetry, the only irreducible representation which can have a continuous order-disorder transition has a three component order parameter with the wavevectors $\mathbf{q}$, $\mathbf{k}_1$ and $\mathbf{k}_2$ shown in Figure 3. The order parameter ϕ_3 corresponds to the c(2x2) phase [60] and, because (2x1) and (1x2) phases do not occur, $\phi_1 = \phi_2 = 0$. The possibility of two independent sets of atomic displacements along <11> or <1T> directions means that ϕ_3 has two components

$$\phi_a = A_a \cos \mathbf{q_a \cdot r}$$

and

$$\phi_b = A_b \cos \mathbf{q_b \cdot r}.$$

The corresponding LGW Hamiltonian has the form

$$H_{LGW} \propto (r/2)(\phi_a^2 + \phi_b^2) + u(\phi_a^2 + \phi_b^2)^2 + w(\phi_a\phi_b)^2.$$

The third term breaks the isotropy of the first two and restricts the displacements to lie along either the <11> or <1T> directions. This restriction to orthogonal directions is refered to as the "cubic anisotropy". The coupling coefficient w must be positive to insure that H_{LGW} has a minimum value when the displacemants go to zero at the critical temperature. This Hamiltonian is identical to that of the XY Model with cubic anisotropy universality class [21,22]. This class is interesting because its critical exponents are non-universal, that is, they depend upon the strength of the interactions as indicated by the results of model calculations [61] shown in Figure 6. The value of β is predicted to be very near the two-dimensional Ising value 1/8 except for very small w; β diverges rapidly to infinity at w = 0.

Wendelken and Wang [59] have measured $\beta = 0.14 \pm 0.04$, which is within experimental uncertainty of the Ising value indicating that the coupling coefficient w is not too near zero. They have also measured β on a surface oriented 3.25° off the (001) surface to produce 3.0 nm wide terraces with step edges parallel to [010]. These finite size effects caused the critical temperature to incresase to 217 K and β to decrease to 0.05 ± 0.01. This large change in β illustrates the importance of finite size effects in surface studies and emphasizes the need for a well-characterized substrate.

Mo(001) undergoes a similar transition [62] but its critical behavior has not been studied in detail.

4.1.3. Other Clean Surface Reconstruction Systems.

Order-disorder phase transitions have been observed for several other clean surfaces. However, these transitions are either believed to be first order or to mirror an underlying bulk transition.

Bennett and Webb [47] have shown that the clean Si(111)(7x7) surface undergoes a reversible order-disorder transition with $\beta = 0.11 \pm 0.02$ and $T_c \sim 1140$ K. However, a consistent interpretation of these results in terms of a continuous transition was not possible since the data showed no indication of the expected broadening of the line profiles due to critical fluctuations. This transition is not expected to be continuous. The Si(111)(1x1) surface has C_{3v} symmetry with six classes of operators. Thus, the order parameter of the (7x7) phase can contain at most six components if the transition is to be continuous. However, as pointed out by Willis [60], the order parameter may have up to 48 components; i.e. the number of new diffraction beams per (1x1) substrate beam. Although the actual number of components may be smaller than 48, it seems unlikely that the Landau rules can be satisfied for Si(7x7).

The bulk disordering of Cu$_3$Au is a classic example of a discontinuous transition. A transition also takes place in the same temperature range on the (001) surface but with modified form. This surface transition has been studied several times since the early experiments of Sundaram et al. [52] yet, other than the fact that it accompanies the bulk transition, its detailed character remains uncertain. Jamison et al. [63] and Alvarado et al. [64] provide evidence using polarized LEED that this transition is continuous although the detailed intensity and polarization variations they report are substantially different. On the other hand, the data of McRae and Malic [65] point to a discontiuous transition. Theoretical models by Kumar and Bennemann [66] indicate that either case can be possible depending upon the details of the interatomic potentials near the surface. Substantial work needs to be done to clarify the experimental situation.

The critical behavior of the surface magnetization of the Ni(001) surface is another surface phase transition whose critical behavior follows the bulk transition. The critical exponent β has the value 0.825 and lies between the three dimensional Ising and XY Model values [67].

4.2. Continuous Transitions in Adsorbed Overlayers.

4.2.1. O/Ni(111) p(2x2)

The order-disorder transition of the O p(2x2) phase on Ni(111) is the first example of critical exponent determination for a chemisorbed layer [68-70]. Line profiles of the (0,1/2) beam were measured with an external photometer. The profiles were analyzed using a method similar to that described above for Au(110) except that the effects of the broader instrument response function were included. The resulting exponents are shown in Table 2. The lattice of adsorption sites on Ni(111) has triangular symmetry since the oxygen atoms are known to occupy the threefold hollows so that, at first glance, Table 1, this transition is expected to be in the so-called four-state Potts universality class [21,22].

The measured exponents are clearly much larger than the predicted values. In fact, within the experimental uncertainties, they agree with the Ising exponents. Roelofs et al. [68] were able to show that this discrepancy cannot be explained by the logariathmic corrections to the four-state Potts model which were not included in their original analysis of the data. Several explanations for this have been suggested. Schick [71] pointed out that there are two types of adsorption sites of the (111) surface of a face-centered-cubic crystal--those which would be occupied by the next layer of nickel atoms in the normal abcabc ... stacking sequence and those sites which would be hexagonal-close-packed-like with ababcabc .... The four-state Potts model results only if there is a significant energy difference between these two types of sites. If there is no difference, the sites become equivalent forming a honeycomb lattice. In this case, the transition could be in the Heisenberg model with cubic anisotropy until very near T_c where 4-state Potts behavior would dominate. The Heisenberg model with cubic anisotropy has variable exponents which can have values very near those of the Ising model [72].

A second explanation is that defects in the form of impurities, random defects and edge effects can change the critical behavior from that expected for a perfect infinite system [73,74]. For example, calculations have demonstrated that random impurities dramatically change the exponents to values in agreement with the measurements [75]. The nickel substrates used in these experiments were more carefully prepared than is typically the case in surface experiments making it unlikely that more perfect surfaces can be easily obtained without using more sophisticated X-ray orientation methods. Furthermore, in any real system the mosaic structure and equilibrium concentration of vacancies and self-adatoms can be substantial. Thus, if this latter explanation is true, critical exponents extracted from surface systems would have to be interpreted with great caution.

A third explanation is that other effects such as multiple scattering, thermal diffuse scattering or variations in the effective nickel scattering factors are

important [40]. Repeating the analysis at significantly different diffraction geometries provides one way to test for these effects.

4.2.2. Ag(110) c(2x2) Cl.

Chlorine occupies the fourfold hollow sites on the square lattice of the Ag(100) surface and forms an ordered c(2x2) structure [76]. The order-disorder transition should thus be in the Ising Universality Class. A recent experimental study by Tayler et al. [77] shows that this indeed seems to be the case. However, only one critical quantity was extracted from the data.

The only critical line observed for this system is that separating the low coverage disordered phase from the higher coverage c(2x2) phase. Since this line is nearly vertical, Cl/Ag(100) is an example of a system in which a critical coverage, θ_c, rather than a critical temperature, must be measured. As discussed by Tayler et al., the critical behavior of the intensity is decribed by an effective exponent $\beta/(1-\alpha)$. The value of $\beta/(1-\alpha)$ is found to be 0.12 ± 0.03 in good agreement with the Ising value, Table 2. The critical coverage is $\theta_c = 3.94 \pm 0.007$ independent of temperature up to the onset of Cl desorption. This value is slightly higher than the hard square Ising model value of 0.368 probably due to a small next nearest neighbor repulsion.

Although the expected broadening of the line profiles was observed, the critical exponents γ and ν were not extracted from the data. Since there is some disagreement about the behavior of Cl on Ag(100) [76], determination of these additional exponents is important to confirm its universality classification.

4.2.3. W(110) p(2x1)-H and p(2x2)-H.

Lyuksyutov and Fedorus [78] have estimated a value of β from their measurements of the T-dependence of the fractional order diffraction beams on this adsorption system. They do not report line profile measurements and did not attempt to account for the effects of instrument response or critical fluctuations in their analysis. In order to account for possible finite size effects on their results, they assumed a Gaussian distribution of T_c with a width ΔT in their fits to the measured data. In total three parameters (T_c, β, ΔT) were used in the fits. The large errors in the values of β, Table 2, are due to the strong interdependence of I_{LRO} on β and T_c.

The bonding site of H on W(110) is the subject of some controversy since it has only recently been realized that the substrate reconstructs [79]. If it is assumed that H bonds either linearly on top of W atoms or in equivalent long bridge sites, the

20

symmetry is the same as the bulk, c2mm, and these phase transitions are predicted to belong to the XY Model with cubic anisotropy univesality class. As shown in Figure 6, β should be very near the Ising value 0.125 unless the cubic interaction w is very small. β diverges rapidly to infinity at w = 0. Lyuksyutov and Fedorus's low coverage values are in agreement with this model but the critical exponent values seem too high.

Substantially more work is required on this system. In particular, a more complete experimental study of the critical behaviors essential. Since the fractional order beams due to ordered H overlayers are weak even in the presence of substrate reconstruction, such studies are expected to be difficult. Measurements should concentrate near the so-called Kosterlitz-Thouless point where the critical lines separating the (2x1), (2x2) and fluid phases come together.

4.2.4. Oxygen on W(112).

Wang and Lu [80] have studied the critical behavior of the p(2x1) structure formed by oxygen chemisorbed on the W(112) surface. The critical exponents extracted from the experimental data, Table 2, support the Ising universality classification obtained from symmetry arguments. Above T_c, measured profiles were fit in the way described above for Au(110) [16] to obtain γ and ν. The resulting values, $\gamma = 1.79 \pm 0.14$ and $\nu = 1.09 \pm 0.11$, are in good agreement with the Ising values of 1/8 and 1, respectively. The exponent $\beta = 0.13 \pm 0.01$ was extracted without correcting the data for the instrument response using a method proposed by Lyuksyutov and Fedorus [78]. This method cannot be applied too near T_c since it does not account for the contributions due to fluctuations. This greatly restricts the range of t; Wang and Lu found 0.016 < t < 0.083. A reevaluation of their data using the BER method [15] should also allow the exponent α to be determined.

As is the case for most experimental studies of phase transitions, data was reported for only a single fractional order beam.

4.2.5. Group 1a and 2a Metals on W(011) and Mo(011).

Fairly extensive studies of the phase diagrams of the Group 1a and 2a metals adsorbed on the (011) surfaces of W and Mo have been carried out [1,81-83]. Ba adsorbed on W(011) is a typical example [81]. A series of coincidence phases is observed at low coverages and undergo first-order transitions upon heating. However, a commensurate (3x2) phase at $\Theta \simeq 0.83$ appears to disorder continuously upon heating with a critical temperature near 125 K. Fedorous and Gonchar [81] measured the

21

intensities of fractional order beams during this transition using a detector aperature approximately equal to the full-width at half-maximum of diffraction beams in the well-ordered low-temperature (3x2) phase. They erroneously attempted to extract the critical exponent ß from this data by ignoring the effect of their poor instrumental response function. An appropriate analysis should use the BER method [16]. We have applied such an analysis to the data in Figure 3 of reference 81 using the assumptions described in reference 55. We find that α is near zero for the (3x2) order-disorder transition indicating that it must belong to either the simple Ising or XY with cubic anisotropy universality classes.

4.2.6. Other Adsorbate Systems.

The phase diagrams of a large number of other adsorbate systems have been characterized. A few of these seem to have continuous transitions and should be the subject of future studies. Some examples include: Se/Ni(001) [5], S/Ni(111) [84], Te/Ni(111) [85], Bi/Cu(111) [86], H/W(001) [60], H/Mo(001) [60], S/Mo(110) [87].

4.2.7. Two Component Adsorbed Layers

Multi-component adsorbed layers should offer even richer behavior than the single component systems described above. However, the need to control two adsorbate coverages and the large range of relative coverage possibilities makes such studies difficult.

Lad et al. [84] have studied O and S adsorbed on Ni(111) to a total coverage of one-half. A mixed-phase coexistence region with O-rich and S-rich c(2x2) domains forms at low temperatures and transforms into a c(2x2) phase with substitutional disorder as T is increased. At higher temperatures, the system is disordered.

5. SYSTEMATIC BEHAVIOR

Enough phase diagrams have been determined to begin examining the systematic variations between them. This offers the possibility of much more stringent tests of theoretical models than is possible in an in-depth study of a single adsorbate-substrate system.

The chalcogens O, S, Se and Te adsorbed on Ni(111) have been studied in some detail [69,84,88]. The substrate bonding is believed to be similar in each case but the adsorbate-adsorbate interactions will vary. Figure 7 shows the partial phase

diagrams for O, S and Te. Surprisingly, these diagrams differ significantly. For example, a p(2x2) phase is the ordered phase at lowest coverage for O and S whereas Te forms a (2 √3 x 2√3) phase. A(√3 x √3) phase occurs below room temperature for O, is not observed for S and exists only above 700 K for Te. Complex coincidence structures form at high coverages for S and Te while O forms bulk compounds. The precise origins of these complex differences is not understood and offer new challenges to theory.

6. CONCLUSIONS.

This review has attempted to summarize recent experimental studies of critical behavior in continuous order-disorder phase transitions on surfaces. Several points should be emphasized in conclusion.

First, the appropriate proceedures for acquisition and analysis of the diffraction data are only beginning to be understood. Surface preparation methods are relatively crude and important contributions of finite size effects introduced during the sample orientation, polishing and cleaning cannot be ruled out in any of the systems studied so far. As demonstrated in the cases of Au(110) and W(001) the effects on the critical behavior can be significant. This may be the most important problem facing experimentalists interested in critical phenomena on surfaces.

More accurate methods are needed for determination of absolute coverages. None of the methods employed have absolute accuracies better than 10 - 20 percent.

LEED has been the only experimental technique used for quantitative studies of critical exponents. In addition to the problems associated with correction for background and thermal diffuse scattering, which will be common for any diffraction method, the important question of whether multiple scattering changes significantly near a phase transition remains unanswered. Combined LEED and Glancing Incidence X-ray Diffraction measurements carried out on the same system should clarify this point in the near future.

The method of Bartelt et al. [15] which uses averaged LEED intensities to determine the exponent α is not sensitive to multiple scattering. Furthermore, the necessary measurements can be carried out with a low resolution LEED apparatus. This is an important development. It means that even the poorest quality instrumentation can be used to study some aspects of critical behavior in a quantitative way.

Finite size effects and/or instrument quality have so far limited the nearness to which the critical temperature can be approached to a few parts per thousand. This

23

means that higher order terms in the expansions of Equations (8)-(12), which define the critical exponents, might not be ignorable.

Finally, it is curious that nearly all of the surface systems studied so far, Table 2, have critical exponents which are most consistent with those of the Ising universality class. Clearly, the hope of finding real physical examples of all universality classes has yet to be realized. Although progress toward using surface phase transitions as models of two-dimensional critical phenomena has been substantial, numerous problems remain and much work needs to be done before this important subject is placed on a firm footing solidly based on experimental evidence.

In spite of these current difficulties, recent progress has been substantial. Improved techniques will develop rapidly and experimental studies of phase transitions are certain to have an exciting future.

7. ACKNOWLEDGEMENT

8. REFERENCES.

1. A. G. Naumovets and Y. S. Vedula, Surface Sci. Repts. **4**, 365 (1984).

2. M. Grunze, in *Chemistry and Physics of Solid Surfaces VI*, Eds. R. Vanselow and R. Howe (Springer-Verlag, to be published); H. Pfnür, P. Feulner and D. Menzel, J. Chem. Phys. **79**, 4613 (1983); A. Horlacher Smith, R.A. Barker and P.J. Estrup, Surface Sci. **136**, 327 (1984); M. Grunze, P.H. Kleban, W.N. Unertl and F. Rys, Phys. Rev. Lett. **51**, 582 (1983).

3. H. Procaccia and M. Gitterman, Phys. Rev. Lett. **46**, 1163 (1981).

4. R. Kern, G. Le Lay and J. J. Metois, in Current Topics of Materials Science, Vol. 3, Ed. E. Kaldis (North-Holland, Amsterdam, 1979) p. 131.

5. P. Bak, P. H. Kleban, W. N. Unertl, J. S. Ochab, G. Akinci, N. C. Bartelt and T. L. Einstein, Phys. Rev. Lett. **54**, 1539 (1985); J. S. Ochab, G. Akinci and W. N. Unertl, submitted to Surface Science.

6. R.J. Birgeneau and P.M. Horn, Science **232**, 329 (1986); J. G. Dash, Physics Today **38**, 26 (1986); E. Domany in *Inerfacial Aspects of Phase Transitions*, Ed. B. Mustaftschiev (Reidel, Dordrecht, 1982) p. 119.

7. A. Erbil, A.R. Kortan, R.J. Birgeneau and M.S. Dresselhaus, Phys. Rev. B **28**, 6329 (1983); M.S. Dresselhaus and G. Dresselhaus, Adv. Phys. **30**, 139 (1981).

8. P.G. de Gennes, *Physics of Liquid Crystals* (Clarendon, Oxford, 1974).

9. A.W. Adamson, *Physical Chemistry of Surfaces* (John Wiley & Sons, New York, 1976).

10. P. Bak, in *Interfacial Aspects of Phase Transitions*, Ed. B. Mustaftschiev (Reidel, Dordrecht, 1982) p. 317.

11. J. M. Cowley, *Diffraction Physics* (N. Holland, Amsterdam, 1975).

12. C. Kittel, *Introduction to Solid State Physics* (John Wiley & Sons, New York, 1986).

13. G. Ertl and J. Kuppers, *Low-Energy Electrons and Surface Chemistry* (Verlag Chemie, Weinheim, 1974).

14. L.E. Reichl, *A Modern Course in Statistical Physics* (University of Texas Press, Austin, 1980).

15. N. C. Bartelt, T. l. Einstein and L. D. Roelofs, Phys. Rev. B **32**, 2993 (1985).

16. J. C. Campuzano, M. S. Foster, G. Jennings, R. F. Willis and W. N. Unertl, Phys. Rev. Lett. **54**, 2684 (1985).

17. S. K. Ma, *Modern Theories of Critical Phenomena* (W. A. Benjamin, Reading, 1976); H. E. Stanley, *Introduction to Phase Transitions and Critical Phenomena* (Oxford, U. K., 1971); K. Wilson, Sci. American **241**, No. 2, 140 (1979).

18. L. D. Landau, Phys. Z. Sowjetunion **11**, 26 (1937).

19. L. D. Landau and E. M. Lifshitz, *Statistical Physics, Part I* (Pergamon Press, Oxford, 1980) p. 459-471.

20. I. P. Ipatova and Y. E. Kitaev, Prog. Surface Sci. **18**, 189 (1985).

21. M. Schick, Prog. Surface Sci. **11**, 245 (1981).

22. C. Rottmann, Phys. Rev. B **24**, 1482 (1981).

23. P. H. Kleban, in *Chemistry and Physics of Solid Surfaces V*, Eds. R. Vanselow and R. Howe (Springer-Verlag, New York, 1984) p. 339.

24. A. E. Ferdinand and M. E. Fisher, Phys. Rev. **185**, 832 (1969).

25. D. P. Landau, Phys. Rev. B **13**, 2997 (1976).

26. L. E. Samuels, *Matallographic Polishing by Mechanical Methods* (ASM, Metals Park, OH, 1982).

27. W. L. Bond, *Crystal Technology* (John Wiley & Sons, New York, 1976).

28. See for example: J. L. Whitton, G. Kiriakidis, G. Carter, G. W. Lewis and M. J. Nobes, Nuclear Instrum. Methods B **2**, 640 (1984).

29. See for example, P.H. Holloway and J.B. Hudson, Surface Sci. **33**, 56 (1972).

30. See for example: *Electron Spectroscopy for Surface Analysis*, Ed. H. Ibach (Springer-Verlag, Berlin, 1977).

31. M.G. Lagally, to be published in *Methods of Experimental Physics*, Eds. R.L. Park and M.G. Lagally (Academic Press, New York).

32. J. J. Weimer, E. Umbach and D. Menzel, Surface Sci. **159**, 83 (1985).

33. J.A. Davies and P.R. Norton, Nucl. Instrum. **168**, 611 (1980).

34. D.F. Mitchell, P.B. Sewall and M. Cohen, Surface Sci. **69**, 310 (1977); Surface Sci. **61**, 355 (1976).

35. D. E. Clark, PhD Dissertation, Univ. Maine, 1986 (unpublished); D. E. Clark, W. N. Unertl and P. H. Kleban (to be published).

36. T. Engel, in Chemistry and Physics of Solid Surfaces V, Eds. R. Vanselow and R. Howe (Springer-Verlag, Berlin, 1985) p. 257.

37. I. K. Robinson, Phys. Rev. Lett. **50**, 1145 (1983); W. C. Marra, P. H. Fuoss and P. Eisenberger, Phys. Rev. Lett. **49**, 1169 (1982).

38. J. B. Pendry, *Low-Energy Electron Diffraction* (Academic Press, New York, 1974).

39. W. Moritz and M. G. Lagally, Phys. Rev. Lett. **56**, 865 (1986).

40. M. G. Lagally and J.A. Martin, Rev. Sci. Instrum. **54**, 1273 (1983).

41. R. L. Park, J. E. Houston and D. G. Schreiner, Rev. Sci. Instrum. **42**, 60 (1971).

42. D. E. Clark, C. S. Shern and W. N. Unertl, J. Vac. Sci. Technol. (in press)

43. M. G. Lagally, in *Surface Physics of Materials*, V. 2, Ed. J. M. Blakely (Academic Press, New York, 1975) p. 419.

44. M. B. Webb and M. G. Lagally, Solid State Phys. **28**, 301 (1973).

45. R.M. Stern, J.J. Perry and D.S. Boudreaux, Rev. Mod. Phys. **41**, (275 (1969).

46. P. Kleban, G. Akinci, R. Hentschke and K. R. Brownstein, J. Phys. A **19**, 437 (1986).

47. P. A. Bennett and M. B. Webb, Surface Sci. **148**, 74 (1981).

48. K. Liang and W. N. Unertl, private communication.

49. C. J. Davisson and L. M. Germer, Phys. Rev. **30**, 705 (1927).

50. A. U. MacRae, Surface Sci. **1**, 319 (1964).

51. D.E. Taylor and R.L. Park, Surface Sci. **L33**, 125 (1983).

52. V. S. Sundaram, R. S. Alben and W. D. Robertson, Surface Sci. **46**, 659 (1974).

53. D. Wolf, H. Jagodziuski and W. Moritz, Surface Sci. **77**, 265 (1978).

54. P. Bak, Solid State Commun. **32**, 581 (1979).

55. L. Onsager, Phys. Rev. **65**, 117 (1944).

56. M. E. Fisher and R. J. Burford, Phys. Rev. **156**, 583 (1967).

57. P. J. Estrup, in *Chemistry and Physics of Solid Surfaces V*, Eds. R. Vanselow and R. Howe (Springer-Verlag, Berlin, 1985) p. 205.

58. T. F. Felter, R. A. Barker and P. J. Estrup, Phys. Rev. Lett. **38**, 1138 (1977); M. K. Debe and D. A. King, Phys. Rev. Lett. **39**, 708 (1977).

59. J. F. Wendelken and G. C. Wang, J. Vac. Sci. Technol. A **2**, 886 (1984).

60. R. F. Willis, in *Dynamical Phenomena at Surfaces, Interfaces and Superlattices*, Eds. F. Nizzoli, K. H. Rieder and R. F. Willis (Springer-Verlag, Berlin, 1985) p. 126.

61. J. V. Jose, S. Kirkpatrick, L. P. Kadinoff and D. R. Nelson, Phys. Rev. B **16**, 1217 (1977).

62. R. A. Barker, S. Semancik and P. J. Estrup, Surface Sci. **94**, L162 (1980).

63. K. D. Jamison, D. M. Lind, F. B. Dunning and G. K. Walters, Surface Sci. **154**, L451 (1981).

64. S. F. Alvarado, M. Campagna, A. Fattah and W. Uelhoff (to be published).

65. E. G. McRae and R. A. Malic, Surface Sci. **148**, 551 (1984).

66. V. Kumar and K. H. Bennemann, Phys. Rev. Lett. **53**, 2798 (1984).

67. S. Alvarado, M. Campagna and H. Hopster, Phys. Rev. Lett. **48**, 51 (1982).

68. L. D. Roelofs, A. R. Kortan, T. L. Einstein and R. L. Park, Phys. Rev. Lett. **46**,

1465 (1981).

69. A. R. Kortan and R. L. Park, Phys. Rev. B **23**, 6340 (1981).

70. L. D. Roelofs, A. R. Kortan, T. L. Einstein and R. L. Park, J. Vac. Sci. Technol. **18**, 492 (1981).

71. M. Schick, Phys. Rev. Lett. **47**, 1347 (1981).

72. G. S. Grest and M. Widom, Phys. Rev. B **24**, 6509 (1981).

73. L. D. Roelofs, N. C. Bartelt and T. L. Einstein, Phys. Rev. Lett. **48**, 1348 (1981).

74. F. Family, Phys. Rev. Lett. **48**, 367 (1982).

75. M. A. Novotny and D. P. Landau, Phys. Rev. B **24**, 1468 (1981).

76. Y. Tu and J. M. Blakely, Surface Sci. **85**, 276 (1979); G. Rovida and F. Pratesi, Surface Sci. **51**, 270 (1975); M. J. Cardillo, G. E. Becker, D. R. Hamann, J. A. Serri, L. Whitman and L. F. Mattheiss, Phys. Rev. B **28**, 494 (1983); M. Kitson and R. M. Lambert, Surface Sci. **100**, 368 (1980).

77. D. E. Taylor, E. D. Williams, R. L. Park, N. C. Bartelt and T. L. Einstein, Phys. Rev. B **32**, 4635 (1985).

78. I. F. Lyuksyutov and A. G. Fedorus, Soviet Phys. JETP **53**, 1317 (1981).

79. J. W. Chung, S. C. Ying and P. J. Estrup, Phys. Rev. Lett. **56**, 749 (1986).

80. G.C. Wang and T.M. Lu, Phys. Rev. B **31**, 5918 (1985).

81. A.G. Fedorous and V.V. Gonchar, Surface Sci. **140**, 499 (1984).

82. O.V. Kanash, A.G. Naumovets and A.G. Fedorous, Soviet Physics - JETP, **40**, 903 (1974).

83. A.G. Naumovets, Sov. Sci. Rev. A Phys. **5**, 443 (1984).

84. R.J. Lad, A.G. Schrott and J.M. Blakely, J. Vac. Sci. Technol. A **2**, 856 (1984).

85. P. Samanta, C. S. Shern and W. N. Unertl (to be published).

86. F. Delamare and G.E. Rhead, Surface Sci. **35**, 185 (1973).

87. A. Sanchez, J. J. de Miguel, E. Martinez and R. Miranda (to be published).

88. R. Ramanathan and J.M. Blakely, Materials Lett. **2**, 12 (1983).

Figure Captions:

Figure 1: Thermodynamic phase diagram for submonolayers of selenium adsorbed on a Ni(001) surface [5]. The open dots are experimentally determined phase boundaries. The solid lines and vertical dashes mark the phase boundaries. All phase boundaries are believed to be continuous for this system.

Figure 2: Structural models of the ordered phases of Figure 1. The solid dots represent Ni atoms in the surface layer of the (001) substrate. The circles represent Se atoms adsorbed at four-fold symmetric hollows on the substrate lattice.
a) The p(2x2) lattice.
b) The c(2x2) lattice.
c) Selenium-selenium interaction energies. The phase diagram in Figure 1 requires $E_3 < E_2 < E_1$.

Figure 3: a) A (2x1) structure on a square lattice substrate. Two symmetry equivalent domains are shown; their boundary is marked by the dashed line.
b) Surface Brillouin zone for (a). The substrate reciprocal mesh vectors are a_1^* and a_2^*. The zone center is at Γ. The reciprocal vectors k_1 and k_2 describe the order parameters for the two (2x1) domains. The wavevector q describes the order parameter of a c(2x2) structure as shown in Figure 2(b).

Figure 4: Temperature dependence of the components of the diffracted intensity near a continuous order-disorder phase transition. The upper portion shows the intensity due to long-range-order I_{LRO} and the amplitude of the susceptibility $\chi(0,T)$, both measured at the Brillouin zone center. The lower portion shows the angular profiles for temperatures just below, at and just above T_c. Only single scattering is assumed.

29

Figure 5:   Critical behavior of the Au(110)(1x2) order-disorder phase
             transition [17]. (a) The temperature variation of the components of
             the intensity due to long-range-order ($\bullet$) and to fluctuations ($+$).
             The solid line is the behavior predicted by Onsager for a simple
             Ising model [53]. (b) Log-log plots of I_{LRO} ($\bullet$), $\chi(0,T)$ ($+$) and
             $\Delta S_{\parallel}(\frac{1}{2})$ (x) vs reduced temperature. The slopes yield the critical
             exponents ß, γ and υ respectively.

Figure 6:   Schematic phase diagram for the XY model with cubic anisotropy.
             The parameter w measures the strength of the anisotropy; w
             positive corresponds to a (2x2) or (2x1) ordered phase and w
             negative to a c(2x2) ordered phase. Along the order-disorder
             transition line, ß varies continuously. (After reference 61).

Figure 7:   Experimental phase diagrams for O, S and Te adsorbed on Ni(111).
             Dashed lines are first-order transitions and solid lines are
             continuous transitions. (After references 69, 84 and 88).

Table 1

UNIVERSALITY CLASSES IN TWO-DIMENSIONS*

Universality Class	α	β	γ	ν	Examples for Common Lattice Types				
					skew/ rectangular	centered– rectangular/ square	Triangular	Honeycomb	Honeycomb in crystal field
Ising	0	1/8	7/4	1	(2x1), (1x2), c(2x1)	c(2x2)		(1x1)	
XY with cubic Anisotropy	non-universal					(2x2),(1x2), (2x1)			
3–State Potts	1/3	1/9	13/9	5/6			(√3x√3)		(√3x√3)
4–State Potts	2/3	1/12	7/6	2/3			(2x2)	(2x2)	(2x2)
Heisenberg with Cubic Corner Anisotropy	0	1/8	7/4	1				(2x2)	

*After M. Schick, Progress in Surface Science 11 (1983) 245.

TABLE 2

SYSTEM	α	β	γ	υ	$T_c(K)$	References
Au(110)(1x2)	0±0.2	0.13±0.02	1.75±0.03	1.02±0.02	650-713	16,35
Si(111)(7x7)		0.22±0.02	*	*	1140	47
O-Ni(111)p(2x2)		0.14±0.02	1.9 ± 0.2	0.94±0.10	427	68,69
O-W(112)p(2x2)		0.13±0.01	1.79±0.14	1.09±0.11	900	80
H-W(110)(2x1)		0.13±0.06				78
H-W(110)(2x2)		0.25±0.07				78
Ba-W(110)(3x2)	≈0[+]				125	81
Cl-Ag(100)c(2x2)		0.12±0.04**				77

*No critical scattering was observed.

**Quantity actually determined is $\beta/(1-\alpha)$.

[+]See text.

Figure 1

p(2×2)   c(2×2)
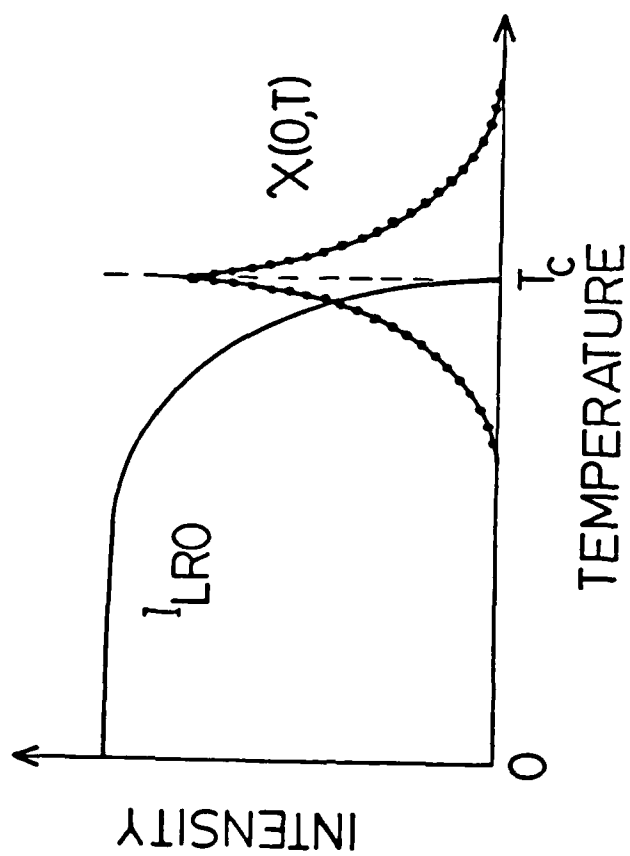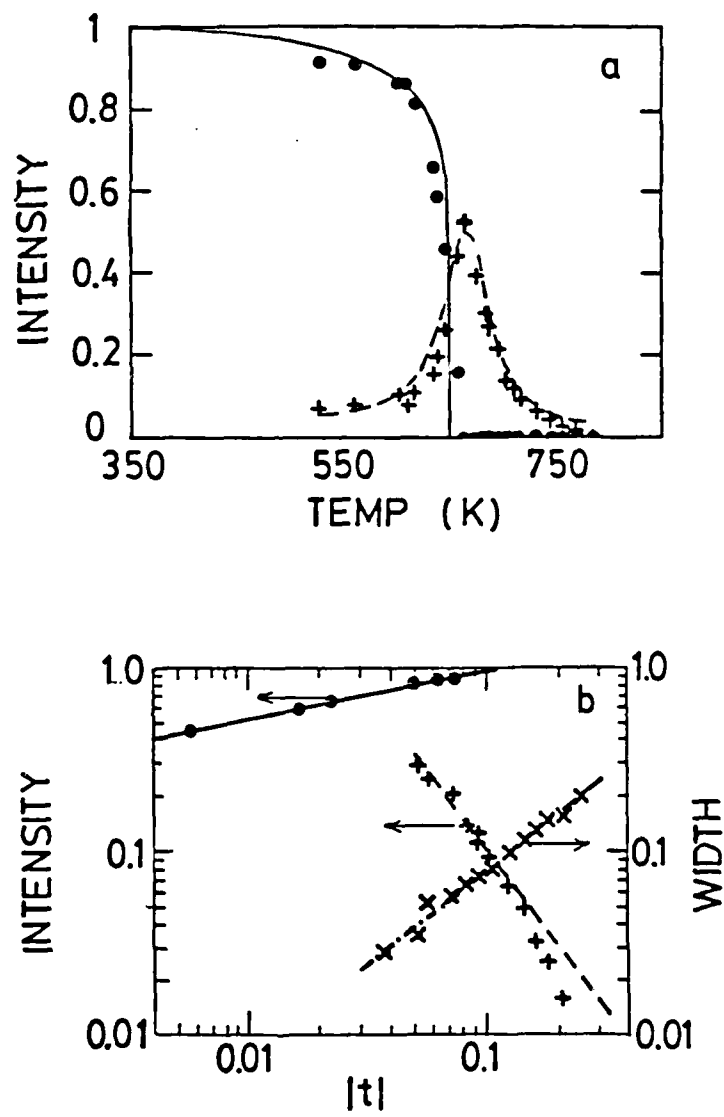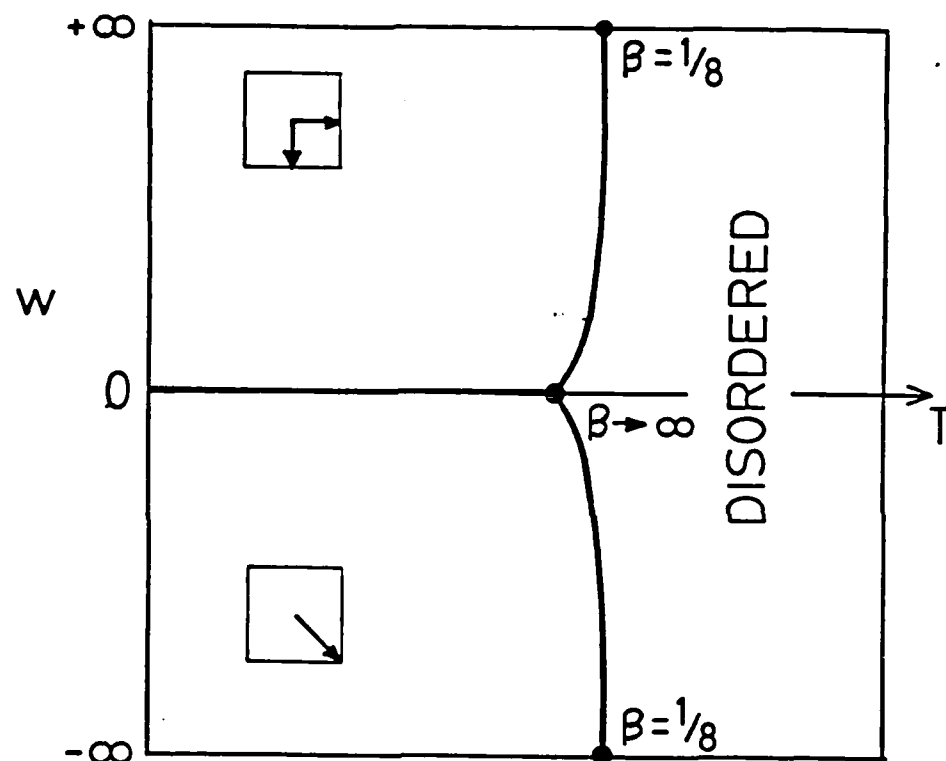
a   b

c
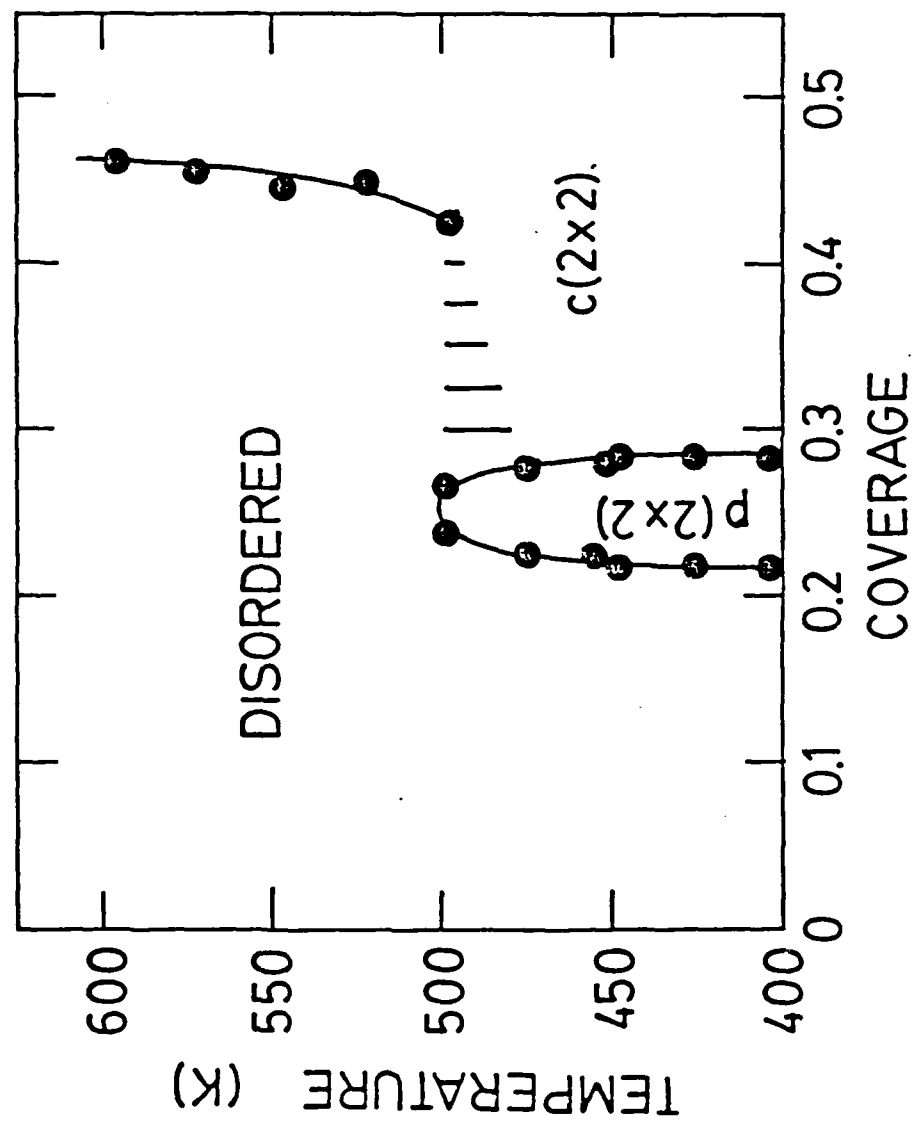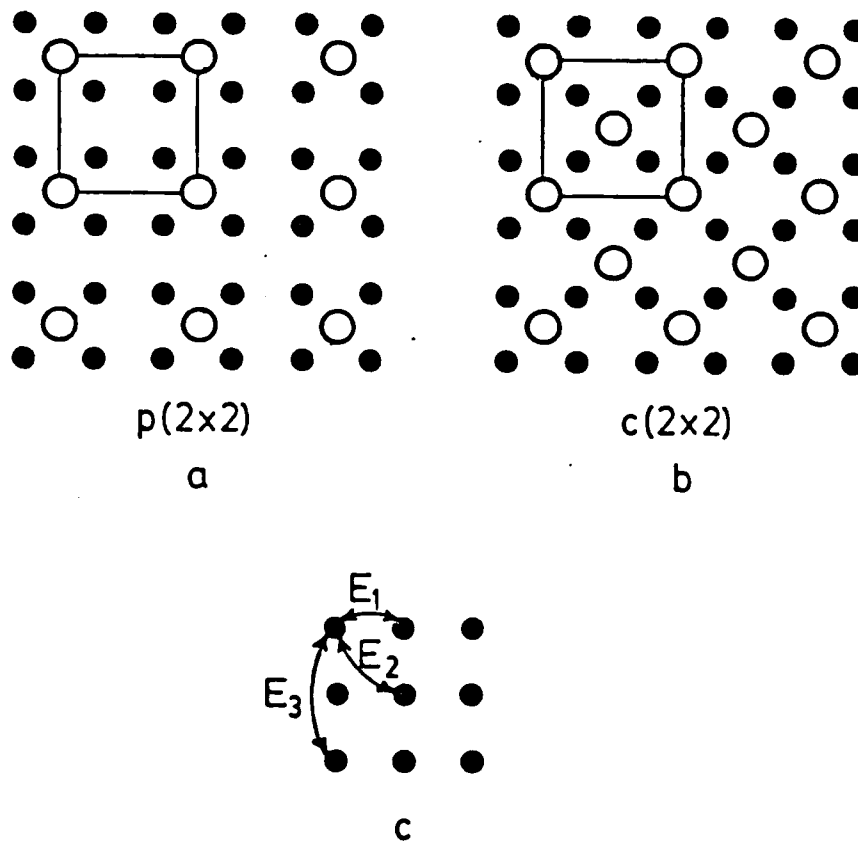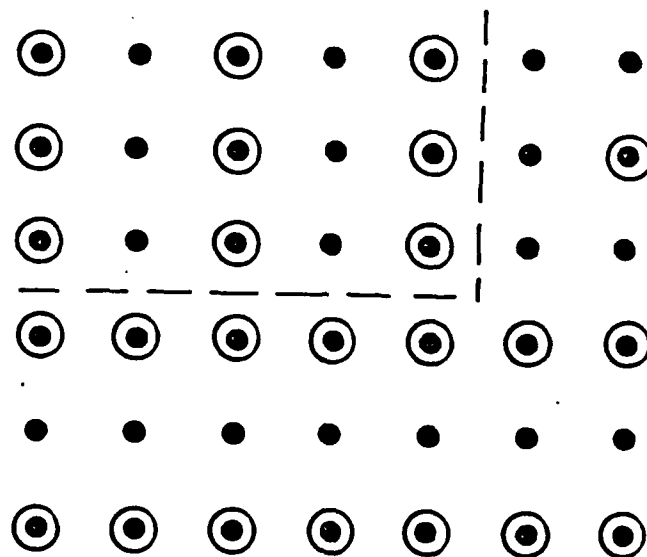
Figure 2

Two Domains (2x1)

(a)

(b)
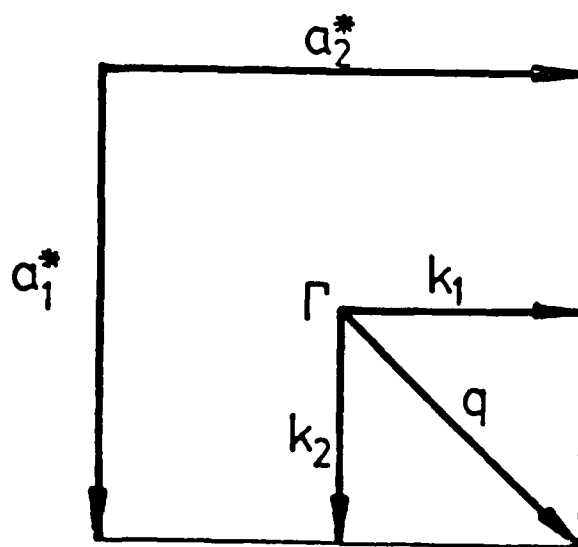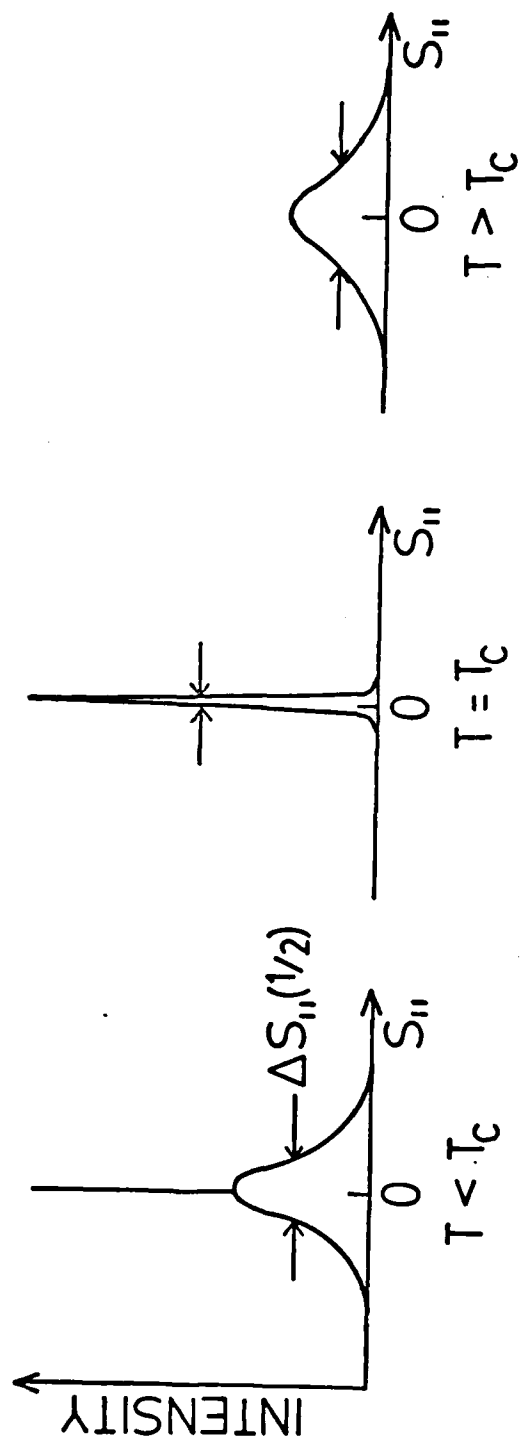
Figure 3

Figure 4

Figure 5

Figure 6

Figure 7

END
DTIC

7 - 86